Journal of Structural Geology 30 (2008) 854–867

Contents lists available at ScienceDirect

Journal of Structural Geology

journal homepage: www.elsevier.com/locate/jsg

The geometry and emplacement of conical sandstone intrusions

Joe Cartwright [a,*], David James [a], Mads Huuse [b], William Vetel [a], Andrew Hurst [b]

[a] 3DLab, School of Earth, Ocean and Planetary Sciences, Cardiff University, Main Building, Park Place, Cardiff, CF10 3YE, Wales, UK
[b] University of Aberdeen, Department of Geology & Petroleum Geology, Kings College, Aberdeen, AB24 9UE, UK

ARTICLE INFO

Article history:
Received 23 July 2007
Received in revised form 20 March 2008
Accepted 27 March 2008
Available online 11 April 2008

Keywords:
Sandstone intrusion
Emplacement
Seismic
Conical

ABSTRACT

Conical sandstone intrusions with a geometry comparable with that of many igneous sills have been identified using 3D seismic data from large areas of the North Sea and Faeroe–Shetland Basins. These intrusions are of reservoir scale, ranging from 100 to 2000 m or so in diameter, 50–300 m in height, and 1–80 m in thickness (aperture). They are concentrated in specific stratigraphic intervals in the Cenozoic fills of both basins. Two geometrical end members are recognised and defined here: 'apical cones' and 'flat-based bowls'. The former consist of inward dipping conical inclined sheets meeting at a prominent apex and the latter of similarly dipping discordant margins climbing from the edges of a concordant sheet. Both end members are associated with domal folds that are interpreted as resulting from the hydraulic elevation of the overburden during intrusion, and which are analogous to similar structures associated with bowl-shaped igneous sills. Measurements of aperture (ω) versus distance exhibit systematic relationships with the structural relief of these folds, offering a potentially predictive method for estimation of sandstone intrusion aperture and reservoir volume prior to drilling. A growth model for these end-member geometries is presented, drawing on existing theory for igneous sill emplacement. Aperture versus distance plots (ω –X) are used to illustrate two contrasting models for aperture inflation during propagation, but these require much further data before any specific growth model can be adopted.

1. Introduction

Sandstone intrusions have been recognised in the outcrop record since the early 19th century, with the vast majority of recorded examples being dykes and sills with apertures (thickness) of less than a metre (Taylor, 1982 and references therein). Most studies of sandstone intrusions have been field-based and descriptive, with only limited attempts made to discuss the processes involved in their emplacement. Notable amongst studies that have explicitly sought a process-based understanding are those presented by Newsom (1903) and Jenkins (1930). More recently, greater effort has been expended on developing a rigorous process framework for the phenomenon of sand intrusion in general (Jolly and Lonergan, 2002; Gallo and Woods, 2004; Jonk et al., 2003). However there is still only a limited treatment of the emplacement mechanics of sandstone intrusions, with emphasis being focused on the conditions necessary for hydraulic fracturing (Cosgrove, 2001; Jolly and Lonergan, 2002).

The lack of a more rigorous mechanical analysis of the process of sandstone intrusion undoubtedly derives from the complex nature of the processes involved. Intrusions of any size require pressure build-up and release in a parent sand body, fracturing of the overburden under generally Mode I conditions, liquefaction and fluidized flow of the sand/fluid mixture from the parent sand body, and multiphase flow to fill the mode I fracture sets (sandstone dykes and sills) (Jolly and Lonergan, 2002; Hurst and Cartwright, 2007). From a mechanical perspective, the occurrence of sandstone dykes and sills provides unequivocal evidence of pure tensile failure and opening at a range of formation depths in the subsurface. Gretener (1980) was the first to recognise the significance of this, correctly identifying their origin as due to hydraulic fracturing, and drawing an analogy with artificial hydraulic fractures induced in wellbore stimulation. His analogy drew on the pioneering theoretical analysis of artificial hydraulic fracturing by Hubbert and Willis (1957), who had suggested that igneous dykes and sills were natural examples of hydraulic fracturing induced by high pressure fluid injection.

Until fairly recently, sandstone intrusions have not generally been considered to have any significance for resource geology such as hydrocarbons, water or minerals, and have therefore been generally overlooked in the large subsurface databases (wells and seismic) that exist in sedimentary basins. In the past decade, the wider availability of 3D seismic data coupled to high resolution well log data has led to the increasing identification of sandstone intrusions in a number of

* Corresponding author.
E-mail address: joe@ocean.cf.ac.uk (J. Cartwright).

0191-8141/$ – see front matter © 2008 Elsevier Ltd. All rights reserved.
doi:10.1016/j.jsg.2008.03.012

petroliferous sedimentary basins (Dixon et al., 1995; Lonergan and Cartwright, 1999; MacLeod et al., 1999; Lonergan et al., 2000; Molyneux et al., 2002; Hurst et al., 2005; Huuse et al., 2004) (Fig. 1). These sandstone intrusions range from a few centimetres up to several kilometres in dimension and exhibit a range of geometries from dykes and sills to lensoid bodies with interconnected sill-like protrusions termed 'wings' (Huuse et al., 2003).

The largest truly intrusive sandbodies thus far recognised are of reservoir scale, i.e. with thicknesses of >40 m, and lateral extents of >1 km. In some cases, recent drilling has indeed shown sandstone intrusions to be acting as hydrocarbon reservoirs in an intrusive form of hydrocarbon trap (Lonergan and Cartwright, 1999; MacLeod et al., 1999), thus highlighting the need to improve our understanding of their genesis to aid in predictive reservoir modelling (Hurst and Cartwright, 2007).

This paper focuses on a specific class of sandstone intrusion, commonly observed on 3D seismic data. This class of conical or bowl-shaped intrusion was first described by Molyneux et al. (2002), but they were previously identified in unpublished reports by geologists for Fina (UK) Ltd. (M. Cope and R. Laver, personal communication, 1992). They have subsequently been identified within Cenozoic successions throughout the North Sea and Faeroe–Shetland Basins (Løseth et al., 2003; Huuse et al., 2004; Shoulders and Cartwright, 2004; Shoulders et al., 2007). Unlike the much steeper dykes, they are exceptionally well imaged by 3D seismic data because they tend to dip at less than 40°.

Recent studies based on 3D seismic imaging of these types of conical or bowl-shaped intrusions have described their basic three-dimensional geometry (Molyneux et al., 2002; Huuse et al., 2004, 2007; Shoulders and Cartwright, 2004; Shoulders et al., 2007). The main aims of this paper are: (1) to refine the existing description of the geometry of conical and bowl-shaped intrusions, (2) quantify their dimensions, and (3) examine their relationship with the host strata, all with an underlying goal of explaining their emplacement. Frequent use is made of analogy with igneous sills of comparable geometry, and the established theoretical framework for igneous sill emplacement is adapted to present a qualitative model for the emplacement of conical sandstone intrusions.

The discussion focuses on differences between two commonly observed end-members of a geometrical spectrum of conical sandstone intrusion types, the apical cones and the flat-based bowls. The paper closes with a discussion of the implications of the intrusions for basin hydrodynamics, as a stimulus for future theoretical analysis of these extraordinary structures.

2. Background and basinal context

Large scale conical or bowl-shaped sandstone intrusions have thus far only been described from the North Sea and Faeroe–Shetland Basins where they are widely distributed in both slope and basin floor environments (Fig. 1). In both basins they are intruded into the fine-grained slope successions of the Palaeocene to Miocene (Molyneux, 2001; Shoulders and Cartwright, 2004). These sediments are clay-rich (typically >50%), dominated by smectite, have extremely low permeability (Yang et al., 2004) and are presently slightly overpressured (Teige et al., 1999). Their pore fluid pressure at the time of intrusion is unknown.

The typical seismic expression of these sandstone intrusions is shown in Fig. 2, as irregular, high amplitude reflections, exhibiting an obvious discordant relationship to the host stratigraphy. When mapped using 3D seismic, these discordant reflections are found to exhibit a spectrum of geometries that differ from any known depositional geometry. This spectrum has two end members: (1) *apical cones*, consisting of smooth to irregular, concave upwards or inverted cones, with fairly sharp, downward facing apices, and (2) *flat-based bowls*, defined by a concordant central sheet and peripheral inclined margins or 'wings' (Fig. 3). This latter end member is similar to the geometry exhibited by many bowl-shaped igneous sills (Smallwood and Maresh, 2002; Hansen et al., 2004; Cartwright and Hansen, 2006). The conical intrusion end member has several possible natural analogues (see Section 6), and similar geometries have also been produced experimentally in laboratory simulations of artificial hydraulic fracturing (Hubbert and Willis, 1957, their Fig. 24; Chang, 2004).

The slope and basin floor sediments that host the intrusions are intensely deformed by polygonal fault systems (Cartwright, 1994;

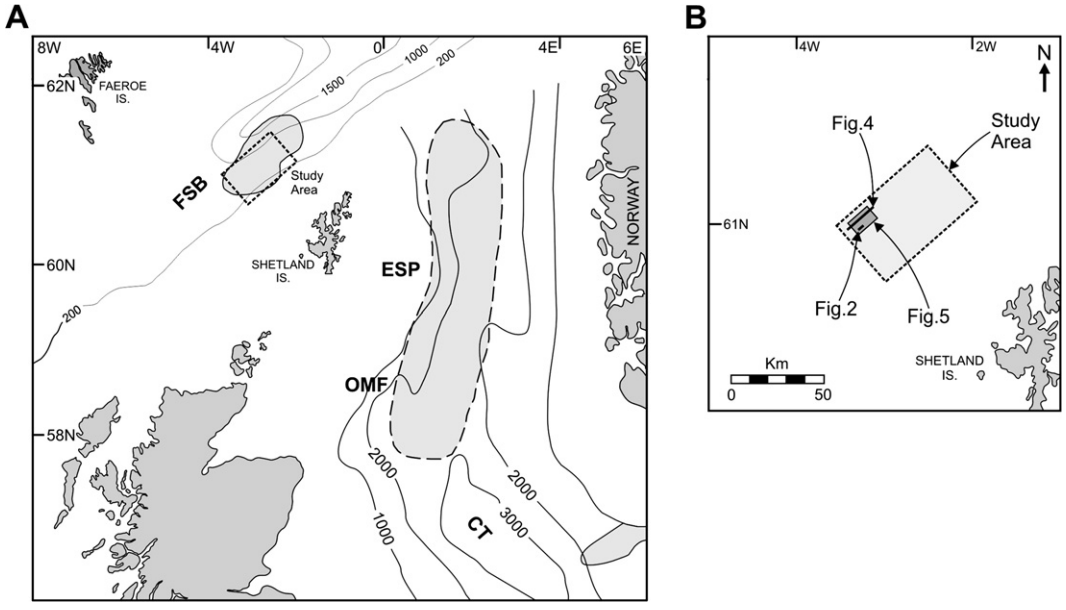

Fig. 1. (A) Location map and distribution of large-scale intrusions in the Faeroe–Shetland Basin (FSB), and North Sea Basin (from Huuse and Mickelson, 2004; Shoulders et al., 2007). Areas in grey tone are regions in which large numbers of conical sandstone intrusions have been observed on 3D seismic data. Rectangular dotted area in FSB is study area from which most of the seismic examples in this paper are taken. Contours in FSB are bathymetry in metres. Contours in the North Sea region are depth in metres to the Top Chalk. ESP , East Shetland Platform ; OMF , Outer Moray Firth ; CT , Central Trough. (B) Location map of study area in Faeroe–Shetland Basin, with location of other figures marked.

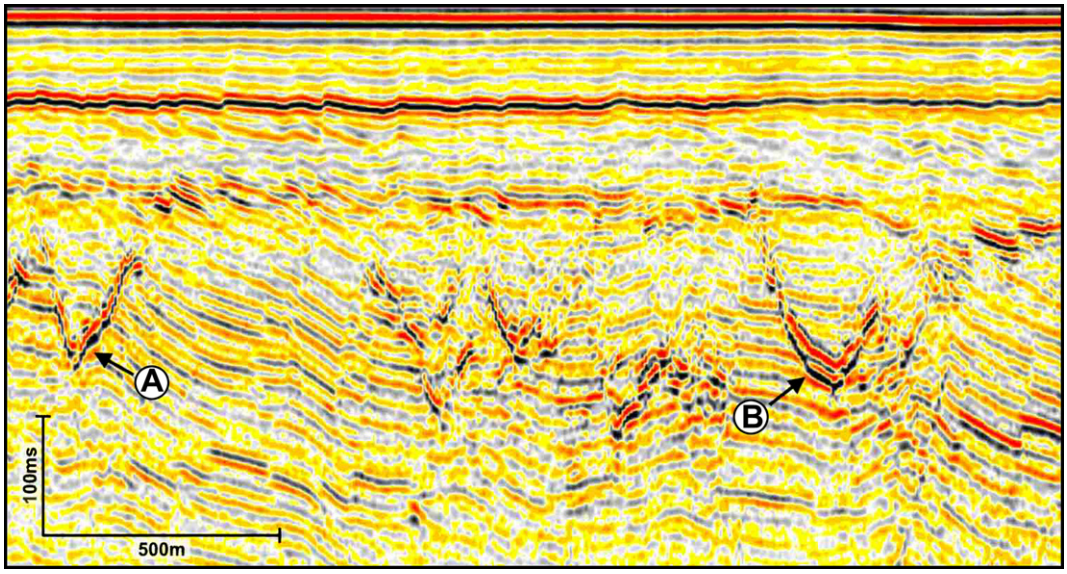

Fig. 2. Seismic expression of conical sandstone intrusions. This profile is from the Faeroe–Shetland Basin, and shows a number of discordant, 'v-shaped' high amplitude reflections with either sharp apices (A) or blunt-based apices (B). These are interpreted as sandstone intrusions within a polygonally-faulted host sequence of Eocene claystone. Note the large variety of cross-sectional geometry, from symmetrical to asymmetrical, singular to composite. Data courtesy of Exxon-Mobil Ltd.

Cartwright and Dewhurst, 1998). Early interpretations of the relationship between the intrusions and the polygonal faults suggested that intrusion occurred along dilated polygonal fault planes (Lonergan and Cartwright, 1999; Molyneux et al., 2002). Huuse et al. (2004) argued that an amalgamation of polygonal faults to form a fully conical linked structure is rarely achieved. Shoulders et al. (2007) supported this view by comparing the dips of conical intrusion flanks with those of polygonal faults at the same depth, and showed that the faults were much steeper than the intrusions. They also described occasional intrusion along fault planes, but mainly cross-cutting of intrusions across fault planes. They argued that the relationship between polygonal faults and the intrusions is exploitative rather than causative.

The use of 3D4C, or multicomponent seismic data (McLeod et al., 1999) and greater availability of well calibrations for lithological control were decisive in demonstrating an intrusive origin for the discordant seismic anomalies in the two basins (Huuse et al., 2007). The well data showed that the intrusive bodies had a typically 'box car' wireline log expression, and were composed of friable, clean sandstone, with variable degrees of calcite cementation (Cosgrove and Hillier, 2000; Duranti et al., 2002; Molyneux et al., 2002; Jonk et al., 2003). Some of the thickest of these borehole-calibrated intrusions are in the central North Sea, in the Chestnut Field, where an intrusion was drilled in the Eocene by well 22/2a-5 and recorded as >40 m thick (Huuse et al., 2004). Well data also show that the largest seismically resolvable intrusions are associated with many smaller intrusions, including dykes and sills (de Boer et al., 2007), so the recognition elsewhere of intrusions from seismic data alone almost certainly implies that they would be accompanied by smaller scale (subseismic) intrusions. It is unknown whether the frequency–size distribution follows a power law relationship, because only a single study to date has attempted quantification of the intrusion array around a large intrusion (Lonergan et al., 2007).

The source of the intruded sands is often poorly constrained, although most likely in the case of the North Sea Cenozoic intrusions to come from highly porous, unconsolidated deep water submarine fan sands of different ages in different sub-basins (Balder Formation – Eocene; Forties Formation, Heimdal Formation – Palaeocene). In the case of the Faeroe–Shetland Basin, the majority of the large scale intrusions are derived from the middle Eocene sand-rich submarine fans developed on the Shetland slope, namely the Strachan and Cuillin Fans. Shoulders and Cartwright (2004) demonstrated that the intrusions emanated directly from this submarine fan system with 3D seismic that imaged the exact position where the intrusions left the parent body on their ascent (Fig. 4). Common to both basins, however, is the likelihood that

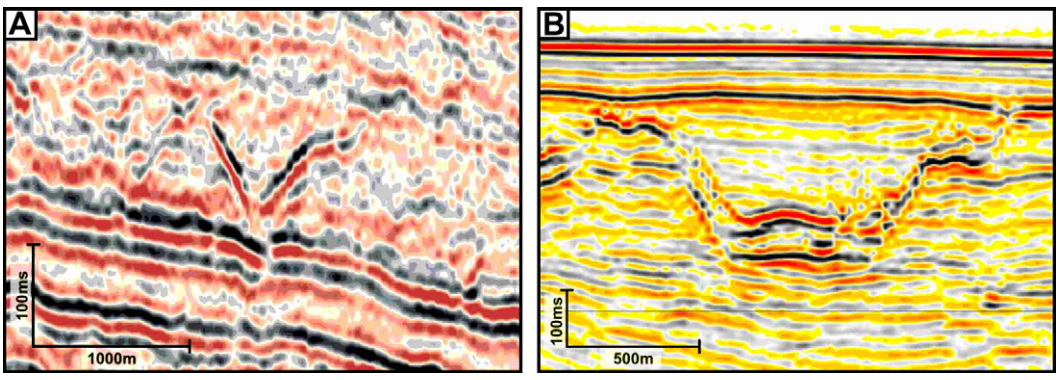

Fig. 3. End members of the spectrum of large-scale conical sandstone intrusions. (A) Apical cones, with sharp apices and inward dipping flanks typically ranging from 20 to 40 ° (from Molyneux et al., 2002). (B) Flat-based bowls, with concordant basal sheets connected to inward dipping flanks similar in scale and range of dip to those flanking apical cones. Data courtesy of Exxon-Mobil Ltd.

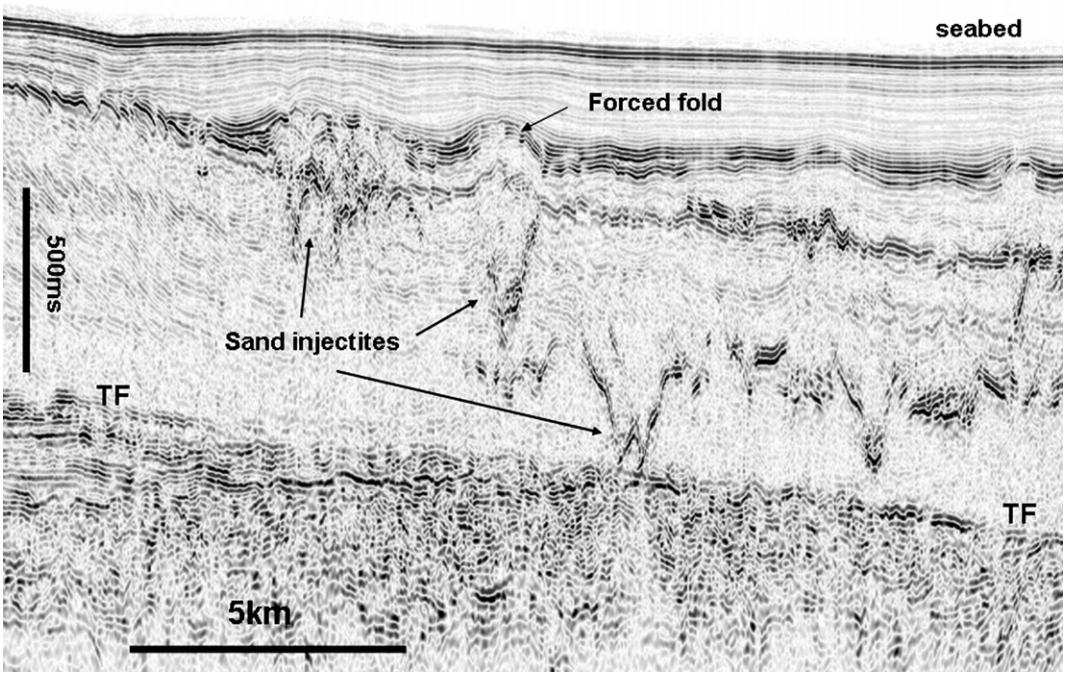

Fig. 4. Seismic profile across the Cuillin Fan in the Faeroe–Shetland Basin, showing discordant amplitude anomalies interpreted as sand injectites emanating from the top of the submarine fan sandstone (TF), and intruded upwards for over 700 m through polygonally faulted Eocene claystones (faults seen clearly on left hand side of the profile). Forced folds at the Miocene unconformity are evidence of the timing of the intrusion event. Data courtesy of Exxon-Mobil Ltd.

parent bodies were very large (10s to 100s of km^3) and very porous, a dual requirement in order to supply the volumetrically large fluidized flows with minimal pressure decline.

3. Stratigraphic distribution

In the North Sea Basin, the vast majority of conical or bowl shaped sandstone intrusions are found in claystones of Eocene age (Molyneux et al., 2002; Huuse and Mickelson, 2004). The full spectrum of geometrical types is observed. The intrusions are most numerous in Lower Eocene host sediments, and then become less frequent in Oligocene and Lower Miocene sediments, where they have been reported only from small areas of the outer Moray Firth Basin (e.g. Quad 16), and the South Viking Graben (e.g. Norwegian Quads 9 and 25) (Molyneux, 2002; Løseth et al., 2003; Huuse and Mickelson, 2004). In the Faeroe–Shetland Basin, the vast majority of seismically resolved sandstone intrusions are apical cones (Fig. 4), and there is only one known example of a flat-based bowl. Intrusions are relatively uncommon in the Palaeocene, very common in the Eocene, and fairly common in the Oligocene, presumably because of vertical separation from the parent sand bodies in each case.

Individual conical or bowl-shaped intrusions cut upwards across a few tens to up to 300 m of statigraphy (Huuse et al., 2007) in both basins. However, in the Faeroe–Shetland Basin, a spectacular example of an interconnected complex of conical intrusions extends for over 700 m vertically from the source to the contemporaneous seabed (Fig. 4) and is distributed over an area of 2000 km^2 (Shoulders and Cartwright, 2004; Shoulders et al., 2007).

4. Intrusion depth

The intrusion depth is potentially an important control on intrusion geometry, and through its relationship to effective stress and pore pressure of the host sediments, can exert a role on the pressure history and storage capacity of the parent sand body (Witherspoon and Neuman, 1972), and on the likelihood of multiphase flow development and gas exsolution during ascent of the intruding fluids (Dake, 2001). To determine the intrusion depth it is first necessary to date the intrusion and define the palaeo-seabed at the time of intrusion. It is not possible to date clastic intrusions directly, except to provide a maximum age based on the age of the intruded sequence. An indirect method for dating clastic intrusions was introduced by Shoulders and Cartwright (2004), using sandstone intrusions in the Faeroe–Shetland Basin as examples. The method is based on defining the palaeo-seabed by recognising onlap onto forced folds that develop by hydraulic elevation of the overburden directly above an underlying conical intrusion (Fig. 4).

In the North Sea Basin, it has not been possible to identify forced folding unambiguously, so there is uncertainty in the palaeo-seabed position at the time of intrusion. The upper tips of many of the conical intrusions generally occur at a common stratigraphic datum over large areas, leading previous authors to suggest that this datum represented the palaeo-seabed (Molyneux et al., 2002; Huuse and Mickelson, 2004). If correct, this suggests that many large conical intrusions in the central and northern North Sea Basin were intruded at depths of up to 500 m, assuming realistic compaction strains compatible with in situ host rock porosity values (Teige et al., 1999). Molyneux (2001), Huuse et al. (2004) and Hurst et al.(2006) have argued that some of these intrusions penetrated close enough to the seabed to supply sand to the seafloor, in the form of 'extrudite' deposits (see also Boehm and Moore, 2002). Recognition of extruded sand has the added benefit of defining the palaeo-seabed at intrusion.

Jolly and Lonergan (2002) used a theoretical approach to derive intrusion depth. This approach requires that the fluid pressure in the parent body and its burial depth are both known at the time of intrusion, which is only rarely the case. Their approach is based on a static model of pressure distribution in the ascending column of fluidized sand, which James (2003) argued is physically unrealistic, so that even were these parameters to be well constrained, the intrusion depths obtained would be of questionable value.

5. 3D seismic interpretation

5.1. Seismic expression

Sandstone intrusions with a conical geometry can only be provisionally identified on seismic profiles from their typically high amplitude reflection character combined with their commonly discordant relationship with the host stratal reflections (Figs. 2, 4). For a conclusive interpretation it is necessary to have direct well calibration. The discordant geometry and the often high amplitude relative to the host sequence are also common to igneous sills (Hansen et al., 2004), so caution must be applied in interpretation of intrusion type in the absence of well data. Sandstone intrusions can either be acoustically 'soft' or 'hard' depending on whether the acoustic impedance of the intrusion is lesser than or greater than that of the host, respectively. The observation of forced fold relationships exhibited by the overburden is an additional aid to interpretation of an intrusive body (see Section 5.4).

5.2. Three-dimensional geometry

The most common geometry of the discordant sandstone intrusions are the apical cones (Fig. 3a). These have sometimes been misinterpreted as channel bodies with strongly erosive, inclined margins (see for example, Newton and Flanagan, 1993) but can easily be differentiated from channelised forms on the basis of planform geometry. Single cones are commonly circular or subcircular in planform, but occasionally are elliptical or shaped like a horseshoe with an open side (Fig. 5). They have been termed 'V' structures or 'V-Brights' informally by Molyneux et al. (2002) and Løseth et al. (2003), respectively, based on their often symmetrical geometry in profile, and their characteristically sharp apex at the junction of the discordant flanks (Figs. 2, 3a). Asymmetrical forms of apical cones are also common, however, and consist of one half of the cone developed to a greater extent than the other. This is often related to local heterogeneity in the host sequence, either through the presence of faults or depositional sand bodies (Fig. 6a).

The discordant reflections forming the cone flanks are often irregular, with several discordant segments linked together by poorly resolved bridging structures, analogous to those described from igneous sills (Fig. 6b) (Thomson and Hutton, 2004). This can either result in a symmetrical or asymmetrical composite structure. Splays into one or more branching reflections are also common towards the upper tips of the discordant reflections (Fig. 6c).

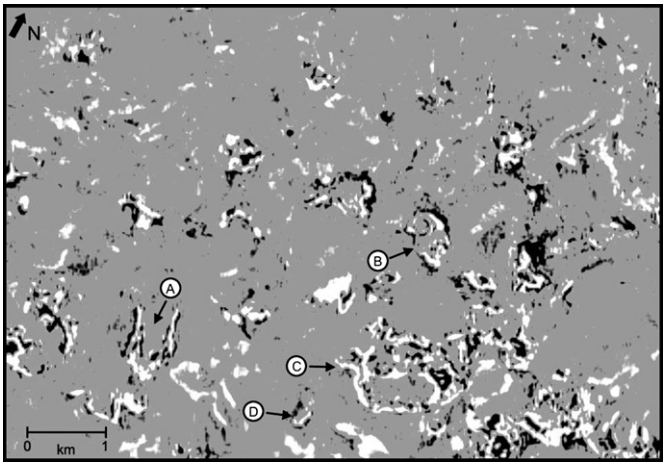

Fig. 5. Time slice through the survey area shown in Fig. 5, showing variation in planform of the sandstone intrusions, from horseshoe shaped (A), to segmented elliptical (B), to multiple composite (C) to singular cones (D). Data courtesy of Exxon-Mobil Ltd.

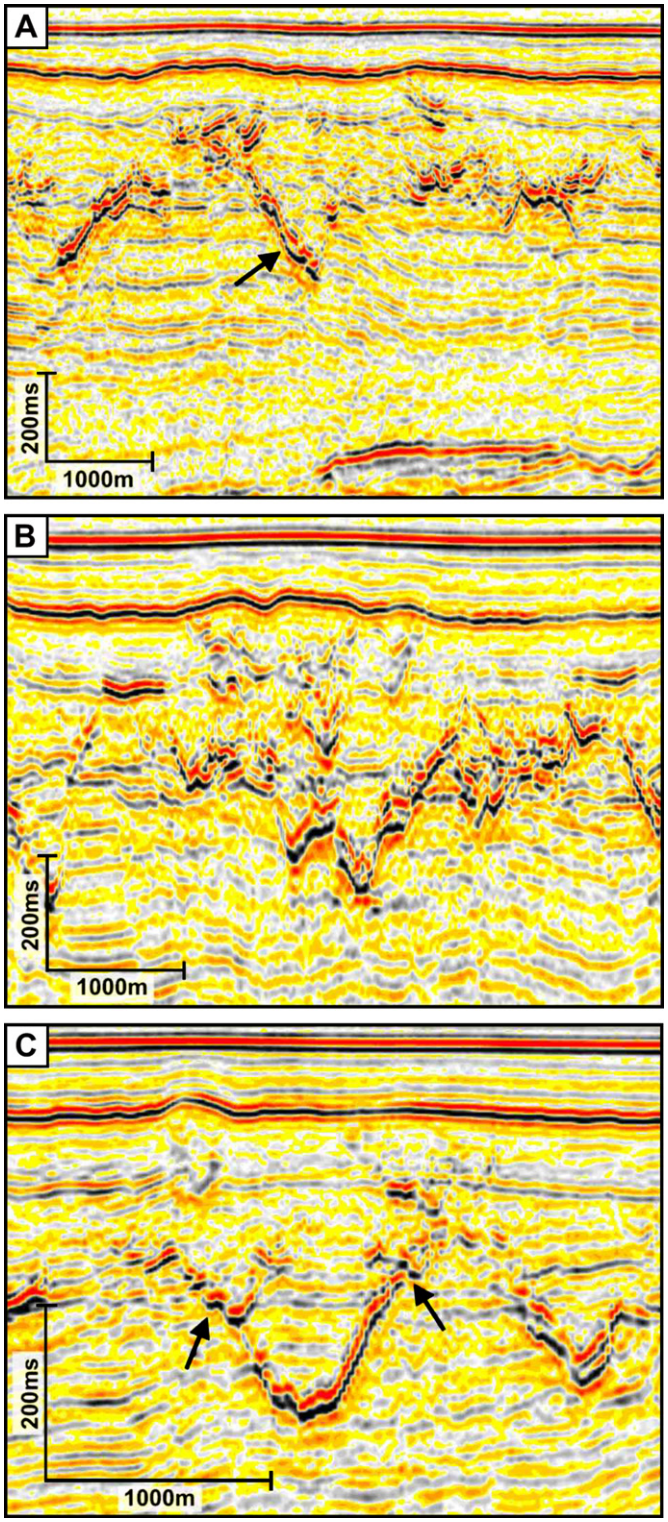

Fig. 6. Detailed seismic expression of apical cones with examples from the Faeroe–Shetland Basin. (A) Example of asymmetric forms, where one flank is better developed because of interactions with pre-existing faults. (B) Example of complex composite form, with many intersections between discordant segments. These can be seen by tracing discordant reflections from pronounced apices upwards into abutting relationships. (C) Example of upward splaying towards the upper tips (arrowed) of a symmetrical form. The splays are easily seen by tracing single high amplitude reflections and noting that they split into two separate reflections. Data courtesy of Exxon-Mobil Ltd.

Mapping of apical cones using 3D seismic data reveals a common form consisting of the basic cone but with variable elements of amalgamation and segmentation. Spatial clustering is not uncommon, and can sometimes be linked to underlying structure, suggesting a control on the feeder system by structural foci such as fold crests or faults (Huuse et al., 2005). Occasionally on the highest resolution data, nested, petal-like segments flaring outwards towards the upper tips, and converging towards the apex or the base can be seen (Fig. 6c). This geometry may be analogous to the fingering observed in igneous dykes and sills (Pollard et al., 1975; Hansen and Cartwright, 2006a). Similar 'petal' geometries have been observed in physical modelling experiments of hydraulic fractures (Hubbert and Willis, 1957), and are found to depend critically on the viscosity contrast between intruding medium and host (Chang, 2004).

At the other end of the geometrical spectrum, flat-based bowls are easily distinguished from the apical cones in having a more concordant central base, flanked on a large proportion of its periphery by a discordant margin (Fig. 3b). These too can exhibit variations involving amalgamation of segments, and splaying at the tips. The discordant margins are generally similar in seismic expression to the flanks of the apical cones.

Resolution is an important factor in the seismic description of the intrusions. Neither the discordant margins of the bowls or the cones are sufficiently sharply imaged to reveal all the details of segmentation, tip structures and intersections that might be expected to be present (cf. Hansen et al., 2004). Frequency content of the seismic data is critical: higher frequency data reveals more irregularity of form because of better vertical and spatial resolution. The deeply buried examples from the North Sea Basin occur in an interval with a dominant frequency in the 20–40 Hz range, yielding a typical vertical resolution of c. 20–30 m (Huuse et al., 2005), whereas the much shallower buried examples of the Faeroe–Shetland Basin occur in an interval with higher dominant frequency and a vertical resolution of c. 10 m (Shoulders et al., 2007) (Fig. 6).

5.3. Dimensions

The dimensions of seismically imaged discordant sandstone intrusions have not previously been systematically recorded. We measured the maximum horizontal and vertical dimension of 51 apical cones from the best resolved interval of intrusions in the Faeroe–Shetland Basin and plotted these against depth beneath the palaeo-seabed (Fig. 7). The palaeo-seabed was taken as a single datum, based on arguments in Shoulders and Cartwright (2007), implying that all the intrusions were emplaced in a single event. This plot shows a surprisingly consistent range of values in dimension across a wide depth range, of 1–1.5 km in diameter and 150–300 m in height. These values compare well with those quoted for conical intrusions in the North Sea Basin (Molyneux, 2001; Molyneux et al., 2002; Huuse et al., 2007). Lateral tips of these intrusions cannot be specified exactly because of resolution limitations, but we estimate the resultant maximum error in dimensions to be $<10\%$. The vertical dimension might be slightly smaller than the maximum value at the time of intrusion, but Shoulders et al. (2007) argued that post-intrusion compaction was very limited because of the <200 m overburden added since the time of intrusion.

The dimensions of flat-based bowls are more difficult to quantify, because it is important to measure both the lateral extent of the concordant base, and the dimensions of the discordant margins. These parameters were recorded for four bowls in the North Sea Basin and one in the Faeroe–Shetland Basin. The dimensions of these five examples base range from 800 m to 2.2 km, with heights of the lateral margin ranging between 130 and 290 m, and lateral extent of the margins ranging from 300 to 800 m. The heights of the discordant margins are likely to have been considerably modified by post-intrusion compaction by up to a factor of two. In all cases, the maximum dimension of the concordant bases exceeds that of the discordant margins. This relationship also applies for flat-based bowls of igneous origin, where measured ratios between the dimensions of bases and margins commonly exceed 2.4 (Trude, 2004; Hansen, 2004).

5.4. Intrusion thickness (aperture)

Measurement of intrusion thickness (aperture) is much more limited by seismic resolution than either width or height. Intrusions in the North Sea Basin are generally only imaged as a single composite reflection because the thickness of the intrusion is often less than the vertical resolution limit. This means that aperture cannot be measured from the seismic data. In the higher resolution examples imaged in the Faeroe–Shetland Basin, however, reflections of opposite polarity (Brown, 2003) are often resolved from the upper and lower contacts of the intrusion, respectively, and hence variation in aperture can be directly measured from depth converted profiles (Fig. 8). The observed reflections compare with forward seismic models of an intrusion of material of higher acoustic impedance into a host sequence of lesser acoustic impedance (Huuse et al., 2007). This opposite polarity relationship is clearly visible, for example, in Fig. 8, where the thickest part of the intrusion is located at the base, and it thins progressively upflank towards the tip, resulting in a wedge-like thickness profile. When the intrusion thins beneath the vertical resolution limit, it is no longer possible to measure aperture directly from the seismic data, because the bounding reflections are interfering with one another, i.e. they are tuned (Brown, 2003).

Aperture (ω) versus distance (X) plots for a selection of four sandstone intrusions are presented in Fig. 9. These were selected from over 30 examples to illustrate the range in patterns observed. This type of plot has not previously been employed in the analysis of sandstone intrusions, but has recently been used to analyse aperture variation in igneous sills (Hansen and Cartwright, 2006b). Ideally, each intrusion should be characterised by a spoke pattern of profiles to capture any variability within the intrusion, but limited variation was found, and hence single profiles suffice to illustrate the general variation of aperture. The error in aperture values is estimated as 5 m from a combination of the positioning or interpretation error and the error due to the 2- ms sampling interval (Brown, 2003). Note that this error is less than the vertical resolution limit of c. 10 m, because this latter limit applies to the separability of reflections generated from adjacent reflecting interfaces, and thus contributes to the lower truncation value in our measurements.

It is important to state that the measured aperture of a sandstone intrusion does not equate to the maximum aperture that existed during active intrusion, because there is loss of pore fluid from the sand/fluid mixture after it comes to a halt inside the fracture, i.e. when it is 'frozen'. The final porosity of the sand fill of the intrusion is always less than the original fluid fraction of the sand/fluid mixture intruding along the fracture. If the final porosity (on 'freezing' of the intrusion), is Φ_f, and the fraction of solid particles of the fluidized sand transported through the intrusion during the peak of the intrusion phase is S, the maximum aperture, ω_{max}, is related to the closure aperture, ω_c, by the following equation:

$$\frac{\omega_c}{\omega_{max}} = \frac{S}{1-\Phi_f} \quad (1)$$

The theoretical upper limit for S in a slurry is approximately 0.5 (Wilson et al., 2006), so if a sandstone intrusion had a closure porosity of 0.4, the final aperture is c. 83% of the maximum aperture. For a more dilute initial slurry of S equal to 0.1 (Gallo and Woods, 2004), for the same closure porosity, this value decreases to c. 16%.

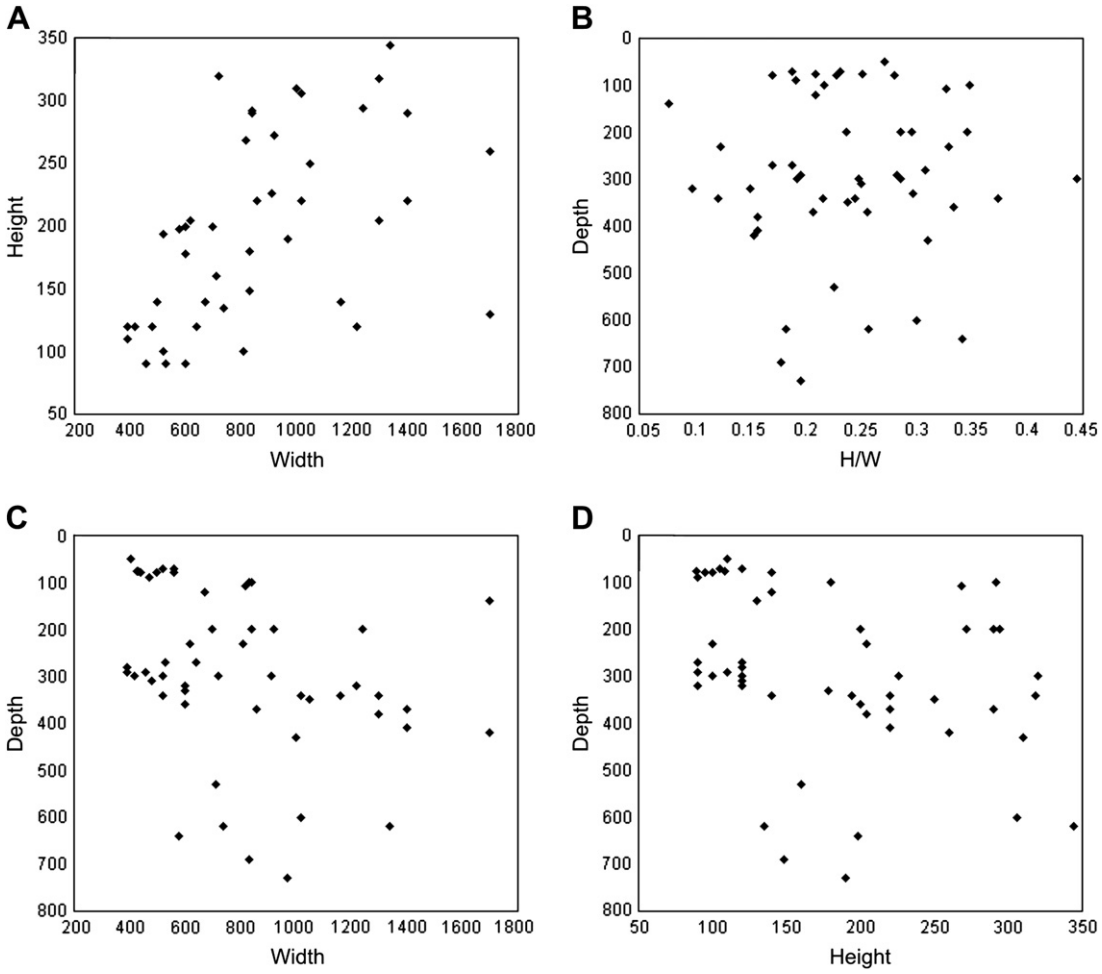

Fig. 7. Plots of apical cone dimensions for 51 intrusions from the Faeroe–Shetland Basin. Depth values are measured from the seabed to the upper tips of the cone flanks and are referenced to a Late Miocene datum interpreted as seabed at the time of intrusion (see Shoulders et al., 2007). Values are in metres. Height is defined as vertical separation from deepest part of the base to the shallowest part of the resolvable tip. Width is measured tip to tip. No strong correlations are seen, except a weak trend of width against height (A).

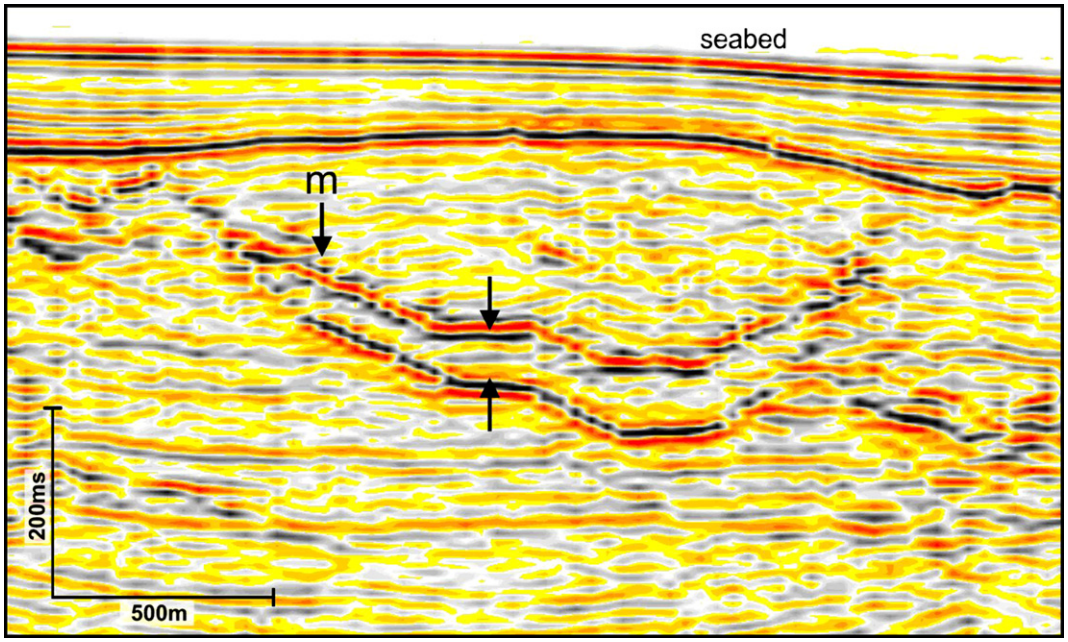

Fig. 8. Seismic expression of a bowl-shaped sandstone intrusion from the Faeroe–Shetland Basin showing the well resolved opposite polarity reflections from the top and base of the intrusion (arrowed). These clearly define the stepped base of the bowl, show the systematic stepping of top and base, and indicate a thinning of the intrusion towards the tips. The details of this wedge-like thinning are partially obscured by multiple reflections (*m*). Also clearly imaged is the forced fold expressed in the strong reflection located c. 100 ms below the seabed. Data courtesy of Exxon-Mobil Ltd.

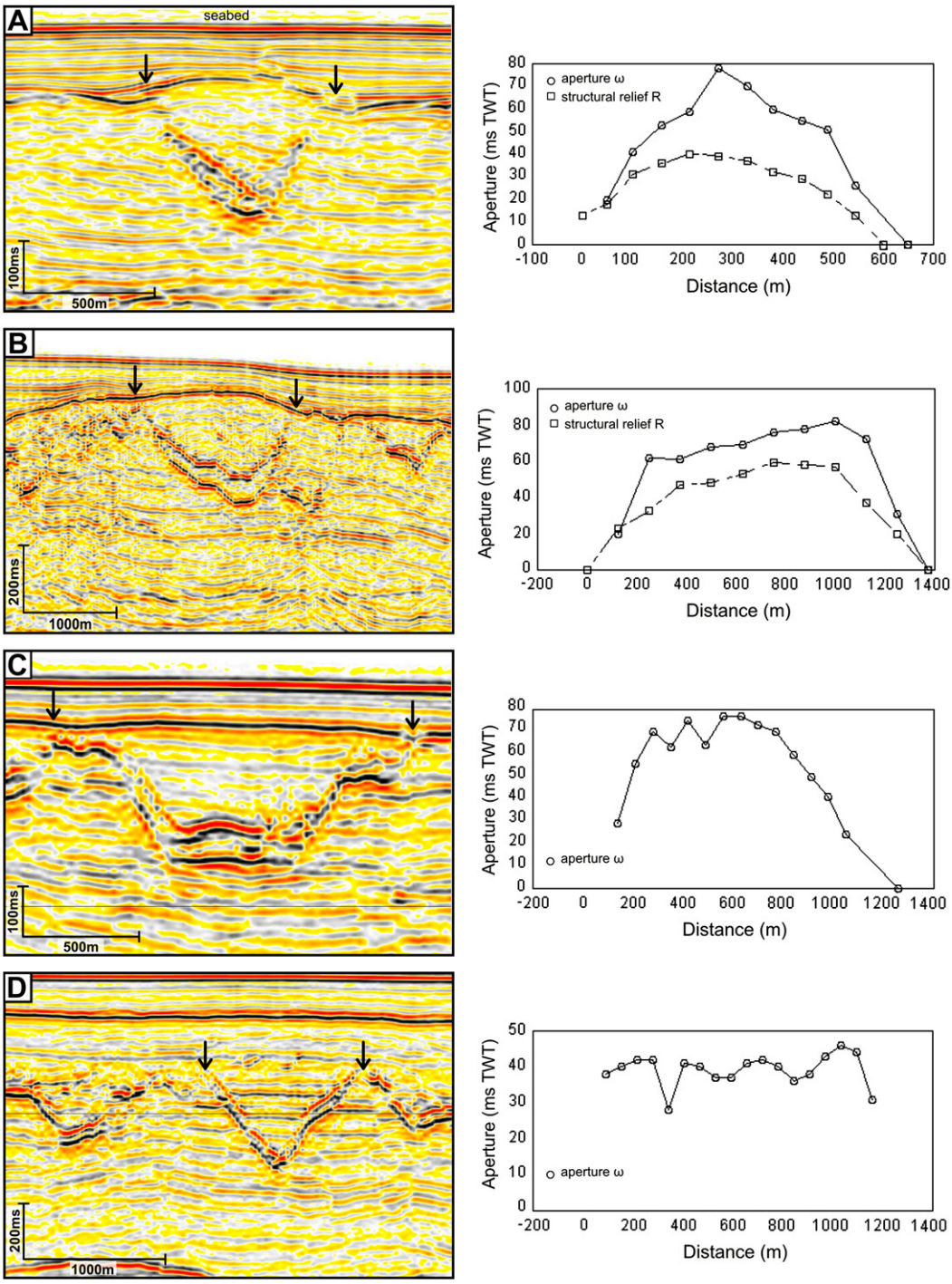

Fig. 9. Aperture (ω) versus distance plots for four representative intrusions from the Faeroe–Shetland Basin, along with measurements of structural relief on accompanying forced folds, where preserved. Aperture values are in milliseconds TWT (1 ms approximately equal to 1 m), arrows on profiles denote start and end points of graphed data. (A) A simple apical cone, with clear wedge-like tapering towards the tips. (B) A stepped flat-based bowl (see also Fig. 10), with a close match between ω and structural relief, R. (C) A classical flat-based bowl, but a probably eroded forced fold. (D) A sharp apical cone, with a tabular distribution of ω, and a flat-topped hydraulic elevation of the overburden, seen in the relative elevations of a pair of prominent reflections inside and outside the structure. Data courtesy of Exxon-Mobil Ltd.

A measured aperture of 16 m would therefore equate to a maximum aperture of 100 m, assuming no loss of porosity following closure. The dependence of the ω_c/ω_{max} ratio on S for a range of Φ_f is shown graphically in Fig. 10. Most measured porosities of apical cones in the North Sea Basin range from 25 to 35%, and bearing in mind some loss of porosity due to burial and cementation post-intrusion, it is likely that closure porosity was of the order of 35–40%. This illustrates that maximum apertures would have been around twice the final value, for an arbitrary value of S of 0.25.

Importantly, the plots of aperture variation across the intrusions shown in Fig. 9 exhibit a tapering geometry towards the tips, notwithstanding their obvious geometrical variation. In all four cases (and on all others we have measured), the discordant flanks have a crudely wedge-like geometry, although the central portions of some intrusions have almost constant aperture, with the tapering wedge being restricted to the near-tip regions (e.g. Fig. 9D). This aperture variation is a persuasive argument in support of a model of upward and outward propagation of the intrusion.

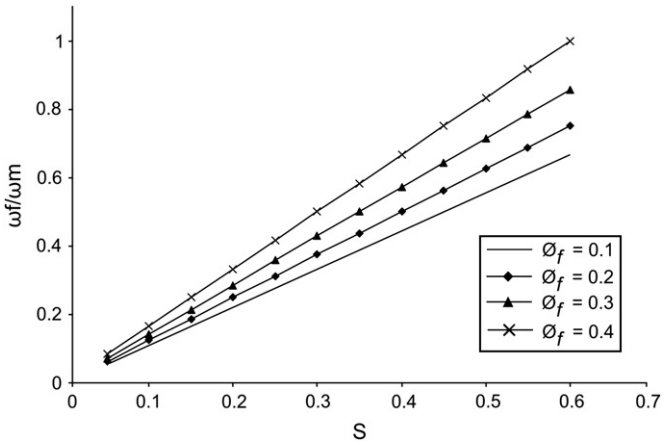

Fig. 10. Graph of aperture ratio (final aperture/maximum aperture) to sand fraction in the fluidized flow for values of porosity at fracture closure (see text).

5.5. Dip

We measured true dips of the flanks of 53 conical intrusions from the Eocene and Oligocene of the North Sea Basin by slicing arbitrary lines through cones mapped on five separate 3D seismic surveys (Fig. 11). The values range from 7 to 33° with a mean value of 22°. The dips flatten slightly with increasing burial depth, probably due to modest compaction of the fine-grained host sediments under the large post-intrusion overburden load (cf. Stuevold et al. (2003) and their explanation of compactional flattening of early formed polygonal faults in the Norwegian Sea).

These dip values compare reasonably with those presented by Shoulders et al. (2007, their Fig. 4) for 267 inverted cones from the Faeroe–Shetland Basin. Their data range from 6 to 57°, with a mean value of 26°. Interestingly, in their case, neither the range nor mean were found to vary with increasing burial depth. Shoulders et al. (2007) argued that there was very limited post-intrusion compactional flattening of the cone flanks. They also argued that the scatter in the dip data was the intrinsic variability that could be attributed to mechanical heterogeneity in the host sequence.

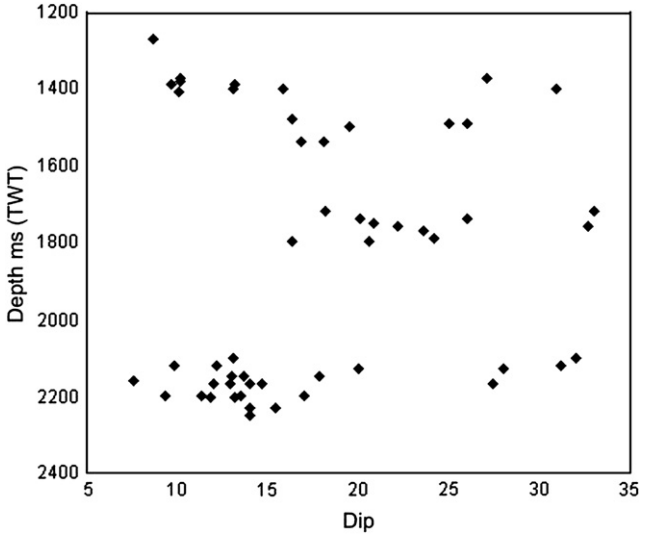

Fig. 11. Plot of true dip of the flanks of 53 apical cones (in degrees) against present day depth (in milliseconds TWT) (1 ms approximately equal to 1 m) from various stratigraphic intervals in the North Sea Basin, showing only a subtle reduction in dip with depth.

5.6. Relationship with the sedimentary host sequence

The intrusion of significant volumes (>1 km^3) of fluidized sand into host sequences raises questions about the nature of the deformation of the host and the specific means by which the intrusion volume is accommodated. In almost all known examples of conical or bowl shaped sandstone intrusions, the host sequence is a dominantly fine-grained succession, which is itself highly deformed by polygonal fault systems (e.g. Fig. 4). As noted earlier, the polygonal faults are occasionally dilationally exploited by the intrusions (Lonergan and Cartwright, 1999) but more commonly the intrusions cross-cut polygonal faults (Huuse et al., 2005; Shoulders et al., 2007). There is no indication on any seismic survey that the space for intrusion was achieved primarily by dilational reactivation of polygonal faults.

Some insight into the accommodation mechanism can be gleaned from the relationship between sandstone intrusions and their host sequences in the Faeroe–Shetland Basin (Figs. 8, 9). Conical intrusions emplaced at shallow level were evidently able to 'jack-up' the overburden to form domal forced folds, suggesting that at least in some cases the space for intrusion was provided by hydraulic elevation (Shoulders and Cartwright, 2004; Shoulders et al., 2007).

The seismic data quality allows the relationship between aperture and structural relief of the forced folds to be examined in detail. Structural relief was measured for a number of these forced folds in the Faeroe–Shetland Basin, and compared with aperture variation across the intrusions (Fig. 9). In all cases, the structural relief varies in crude proportion to the lateral variation in aperture: as the aperture tapers towards the tips, the structural relief decreases towards the regional datum. The structural relief is in all cases some fraction of the aperture, and nowhere is this fraction less than 0.5. In rare cases, the fraction approaches unity.

Similar forced folds have not yet been reported from the intervals hosting the inverted cones in the North Sea Basin, but this may be due to the poorer imaging at deeper burial depths in comparison to the examples from the Faeroe–Shetland Basin. The wide variety of forced folds observed above the sandstone intrusions described here is, however similar to that observed above bowl shaped igneous sills mapped using 3D seismic data (Hansen and Cartwright, 2006b). Domal folds analysed by these authors conform to those predicted for overburden folding above laccoliths (Pollard and Johnson, 1973; Pollard, 1973; Pollard and Holzhausen, 1979; Jackson and Pollard, 1988).

It is quite possible that intrusive forced folding related to sandstone intrusion has been overlooked in the North Sea. For example, forced folding of the type shown in Fig. 9 can be seen associated with flat-based bowl intrusions (e.g. Fig. 13 of Huuse et al., 2007), where structural relief closely matches aperture values calibrated by boreholes. In some cases, the region directly above the main intrusion is pervasively intruded by smaller scale dykes and sills forming an intrusive 'halo' or carapace (Huuse et al., 2005, 2007; de Boer et al., 2007). This suggests that accommodation of the intruded volume was not entirely achieved by simple domal folding, but that the overburden was itself stretched differentially.

6. Discussion

6.1. Mechanical significance of sill geometry

One of the implicit assumptions in the description of the sandstone sills presented above, is that the conical intrusions and the flat-based bowls represent two ends of a spectrum of geometrical forms (Fig. 3). The basis for this is the common occurrence of the former, the widespread though less frequent occurrence of the latter, and the common occurrence of intermediate forms. The

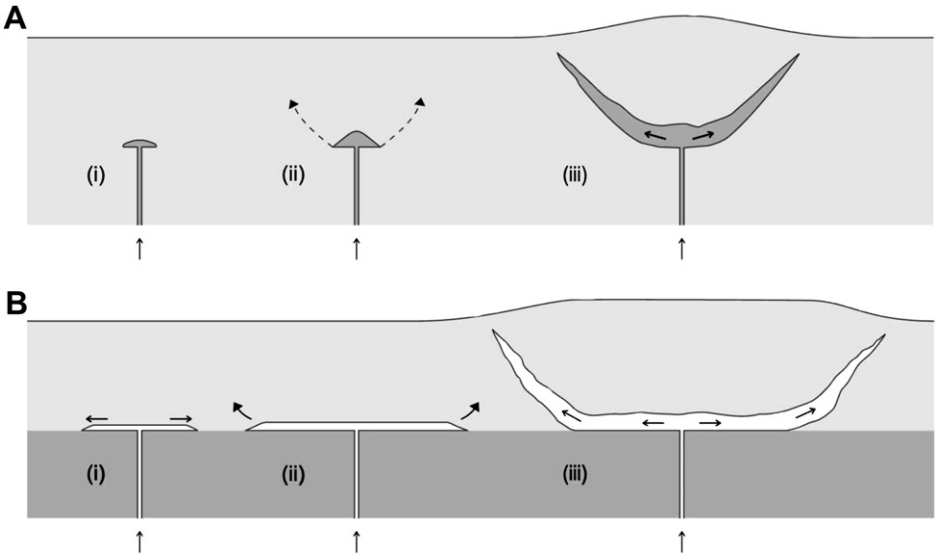

Fig. 12. Schematic model showing the propagation of apical cones (A) and flat-based bowls (B). In (A), a feeder delivers a sand flux to a seed point, where a small laccolith intrusion forms, possibly at a minor competence contrast. This local pressure focus then promotes the propagation of conical fractures in direct analogy with cone sheet formation. In (B), the competence contrast at a boundary is greater, and promotes lateral propagation and not inflation. Once the dimensions of the sill reach a critical value, the fracture interacts with the free surface, and the sill turns upwards towards the surface.

mechanical significance of these two end-members, however, presents two quite contrasting challenges, discussed further below. It is generally assumed in the discussion below that sheet-like sandstone intrusions are true Mode I fractures where the opening direction is initially perpendicular to the fracture walls (Gretener, 1980; Lorenz et al., 1991; Jolly and Lonergan, 2002) and as such are mechanically analogous to igneous dykes and sills (Hubbert and Willis, 1957; Delaney et al., 1986; Lister and Kerr, 1992; Rubin, 1995; Jolly and Sanderson, 1997). Field evidence strongly supports this view, since few previously described sandstone intrusions have been shown to have any significant shear component in their opening direction beyond that of minor obliquity (Taylor, 1982, and references therein).

6.1.1. Flat-based bowls

These have an obvious mechanical explanation that derives from analogous intrusion geometry in igneous sills and sill complexes. Igneous sills mapped in three dimensions are commonly found to have a large, concordant central segment, flanked by a discordant margin around the entire perimeter, consisting of a single or segmented inclined sheet (Trude, 2004; Hansen, 2004). High resolution seismic data show that these marginal inclined sheets taper towards the lateral tips, and often splay into second order segments or lobate fringes (Thomson and Hutton, 2004; Hansen and Cartwright, 2006a).

This observed geometry matches exactly the configuration predicted by Pollard and Holzhausen (1979), for the propagation of sheet intrusions modified by the influence of the free surface. They argued that once a concordant sheet propagated beyond a critical value of the length, $2a$, interaction with the free surface at height, d, above the midpoint of the fracture would result in a non-zero value for the Mode II stress intensity factor, favouring out of plane propagation and upward deflection of the sill tips to form the inclined margins. In this model, the critical point of inception of

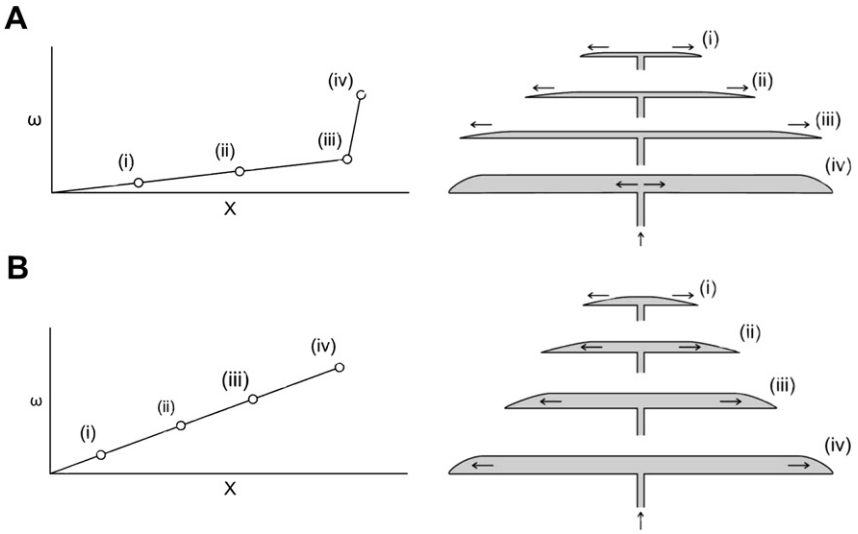

Fig. 13. Two end-member growth models for sandstone sill propagation and inflation. (A) A model of propagation followed by a late stage inflation, with a corresponding ramp in aperture versus distance plot. (B) A self-similar growth model with a constant ratio between aperture and distance.

inclined flanks is for a ratio $d/a < 2$. This general result applies whether the pressure distribution within the propagating fracture is uniform or linearly decreasing towards the tips. The ratio of Mode II to Mode I intensity factors is maximised, however, for the latter case, suggesting that fractures with a pressure gradient are likely to climb at steeper angles towards the free surface. Finally, Pollard and Holzhausen (1979) specifically noted that significant strength anisotropy would likely alter these critical ratios, and probably decrease the tendency for climbing.

More recent formulation of the same process by Fialko et al. (2001) and, for artificial hydraulic fractures by Murdoch (2002), essentially agrees with the two-dimensional model of Pollard and Holzhausen (1979). 2D discrete element modelling using a non-viscous fluid with uniform pressure by Malthe-Sørensen et al., 2004 is also in broad agreement that beyond a critical length for a given depth, the propagation trajectory curves upwards discordantly. Their modelling showed that these 'wing' segments then flattened again as the free surface was approached.

Measurements of the width ($2a$) of the concordant base and depth to the base (d) have only been obtained for five examples for flat-based bowls and yield ratios of d/a of 1.8, 1.8, 2.1, 2.4, and 2.7 (error estimated to be 20%) and are therefore broadly consistent with the theoretical models above. d/a measurements made for igneous intrusions with this geometry are also consistent with theoretical models (Trude, 2004; Hansen, 2004; Polteau et al., 2007).

6.1.2. Conical intrusions

Their distinctive conical geometry with a well-defined apex distinguishes them from flat-based bowls, and the explanation above for flat-based bowls cannot apply, because there is no lateral propagation prior to the development of the discordant margins.

We infer that propagation of these margins was upwards from the apex based on three main arguments. First, the alternative, of radial or downward propagation is unlikely to result in a sharply defined apex. The apical structure in fact points clearly to the location of the feeder position being located at the apex. This argument is supported from observations made of sill complexes where deeper level cones are seen to form junctions with shallower level cones at the apex of the upper cones (Figs. 4,6). This feeder geometry compares closely with that seen in igneous sill complexes where deeper sills feed shallower sills in succession (Hansen et al., 2004; Cartwright and Hansen, 2006). Second, upward and outward propagation is consistent with the outward splaying of the discordant margins (Fig. 6C) and the segmented geometry of many conical intrusions (Fig. 6b). Finally, the common observation that the flanks of the conical intrusions exhibit a crudely wedge-like or tapering geometry (Fig. 9) also argues for upward and outward propagation (cf. Hansen and Cartwright, 2006b).

The arguments presented above allow us to conclude that the apex is the point at which the fluidized sand first begins to intrude outwards, but how is it fed to this point, and why does a circular to subcircular mode I fracture nucleate at this point? Several different types of potential feeder mechanism can be considered. First, the cone-to-cone intersection type of feeders seen in Fig. 6. Second, columnar or pipe conduits have been suggested by Huuse et al. (2004). Last, dykes exploiting polygonal fault planes have been suggested by Molyneux et al. (2002), Huuse et al. (2005), and Shoulders et al. (2007).

Based purely on the geometry of the apical regions, a strong argument can be made for a highly focused delivery of sand (plus fluids) to this position, so whether the feeder is a pipe-like conduit, a deeper-level conical intrusion or a fault-controlled dyke, the flux through this conduit must be sufficient to maintain a open conical fracture that could be up to 50 m or more in maximum aperture with a perimeter length of >3 km. In the case of the interconnected sandstone intrusion complex of the Faeroe–Shetland Basin, this requirement to maintain flux is even more critical, because the array of vertically linked conical intrusions is stacked over a c. 700 m distance, and the shallowest level conical intrusions must be fed from the underlying interconnected cones (Shoulders et al., 2007).

What of the conical geometry itself? Previous explanations of the conical geometry argued for a model of exploitation of previously formed and conically aligned polygonal faults by the intruding sand (Molyneux et al., 2002; Gras and Cartwright, 2002). This early view has been discounted by more detailed mapping of intrusion networks in relation to polygonal fault plane geometry showing cross-cutting of the fault planes by the intrusions (Shoulders et al., 2007). The lack of any systematic exploitation of the randomly oriented polygonal fault planes within the host sequences suggests that whatever the feeder mechanism, it was not specifically linked to dilation of pre-existing fractures (cf. Delaney et al., 1986; Jolly and Sanderson, 1997). It also suggests that the strength anisotropy between fracture or fault planes and the host claystone was negligible and played no part in the development of conical Mode I fracture trajectories.

The propagation of conical mode I fractures can therefore be regarded as a fundamental geometrical property resulting from the emplacement mechanism. The link with the point source located at the apex leads us to infer that this intrusion focus is the critical element in the development of the conical geometry. This link between an intrusion focus and outward propagation of conical mode I fractures away from the focus is directly analogous with the process of cone sheet emplacement above central intrusive complexes or magma chambers. Cone sheets are families of inward dipping sheet intrusions emanating from a common centre or focus (Harker, 1904; Bailey et al., 1924). They can range in dip from subvertical (at the upper tips) to flat-lying (10–20°) (Hills, 1963). The stress distribution above a magma chamber with a cupola shape was first modelled by Anderson (1936) and provides a robust basis for modern analyses of cone sheet emplacement (LeBas, 1971; Johnson et al., 1999; Gudmundsson, 2002).

Modern stress analyses confirm Anderson's calculations of the rotation of principal compressive stresses in the vicinity of the laccolith boundary due to the lithostatic pressured laccolith fill such that σ_{min} is parallel to the boundary (Mandl, 2000). The mode I stress trajectories can therefore be assumed to be governed by the shape of the contact between the overburden and the fluid-filled magma chamber. Taking this model as a mechanical analogy, the intrusion of fluidized sand into a central focus (at the apex), shaped for example like a small laccolith with bulbous margins would then lead to propagation of mode I fractures with conical geometry and inclined into the focus (Fig. 12a). The range of observed dips of conical sandstone intrusion flanks (e.g. Fig. 7) accords well with the range of dips observed for igneous cone sheets (Hills, 1963).

Other natural examples of conical fractures are known to occur, but provide much less satisfactory analogues than cone sheets. The removal of support by evacuation of material at depth, for example, is well documented to produce conical collapse structures, although these most commonly involve shear of the central block overlying the collapsing cavity (Branney, 1995) and as stated earlier, there is no persuasive evidence of shear displacement recorded on any discordant sandstone intrusions. Furthermore, the dip of these collapse structures (O'Rourke and Turner, 1981) is generally much steeper than the range observed here for conical intrusion flanks.

Two other possible analogues are (1) shatter cones associated with impact structures which are known from field evidence to be dilational and contain flow breccias, and (2) spiral fractures associated with high velocity ballistic impacts (Hills, 1963). Both of these are high velocity percussion fracturing processes. It is highly unlikely that an ascent velocity of the fluidized sand of the order of

a few cm^{-1} (Gallo and Woods, 2004; Duranti and Hurst, 2004; Shoulders, 2005), would impart a sufficient stress on the target layer to induce this type of percussive fracture. We conclude therefore, that of the known natural analogues for conical fracture geometry, igneous cone sheets represent the closest fit, and the mechanical analysis developed by Anderson (1936) can be equally well applied to conical sandstone intrusions.

6.2. Conical vs flat-based bowls

The main difference between the emplacement envisaged for the two end-members is that for the conical intrusions, the conical flanks develop without any lateral propagation of a concordant sheet. Different types of feeder are possible for both types of intrusion (e.g. dykes, pipes, faults or deeper sills), so it is possible that the development of the basal concordant sheet is somehow linked to the specific type of conduit involved in each case. We suggest, however, that propagation of the concordant base is more likely if there is a strong mechanical contrast parallel to the layering (Fig. 12b). All the mapped examples of flat-based bowls are associated with major lithological contrasts at the stratigraphic level of the concordant sheet (e.g. Fig. 3b). The existence of a significant strength anisotropy related to bedding is known to favour bedding parallel sills in analogue models of sill and laccolith emplacement (Pollard, 1973; Galland et al., 2003; Kavanagh et al., 2006; Polteau et al., 2008). Whereas, in contrast, recent modelling of hydraulic fractures in homogeneous media under varying confining stresses yielded conical intrusion geometries (Chang, 2004). It is possible, therefore, that where intrusion takes place into a more homogeneous host material, there is no strong tendency for bedding parallel propagation, and a more localised, laccolith-shaped intrusion can develop, leading in turn to cone sheet formation. The tendency for one form or the other to develop might thus be critically dependent on the rheological layering of the host medium.

6.3. Aperture variation and emplacement models

It is tempting to view the observed aperture variation seen for example in Fig. 9 in an analogous way to displacement variation on faults and infer propagation phenomena from the careful study of aperture (Hansen and Cartwright, 2006a). However, it is not clear at present how aperture relates to the propagation history. It is conceivable that propagation of the initial Mode 1 fracture to the final size occurred with very small opening of the fracture, and the final aperture was the product of subsequent inflation to form maximum aperture at the peak pressure conditions of the active intrusion phase, followed by partial collapse once the flow was choked, or pressure of the flow dropped beneath the critical level required to keep the intrusion open (Fig. 13a). Alternatively, it could also be conceived that the growth of aperture proceeded stepwise along with propagation away from the apex, maintaining a critical taper defined by the host material properties (Fig. 13b). These two 'end-member' models of propagation and growth are presented here solely for discussion, and are equally plausible, but since aperture growth with propagation has not been modelled theoretically, it is not clear what factors might favour one model over the other, or indeed other growth models intermediate between these two.

The ratio of structural relief, R, to aperture, ω, as determined where there a forced fold associated with an underlying conical or bowl-shaped intrusion (e.g. Figs. 8, 9) is potentially a useful measure of the effectiveness of hydraulic elevation. This ratio is referred to here as the hydraulic efficiency ratio, with values closest to 1.0 being representative of the most direct coupling between space created for intrusion and forcible uplift of the overburden. A caveat needs to be applied before this measure can be used in prediction of intrusion thickness (sand thickness). The data presented in Fig. 9 could be interpreted in a number of ways: (a) there was some erosion of the folds, so the measured structural relief was not the true relief achieved by intrusive folding, (b) there was some wall-rock abrasion such that aperture of the open fracture was widened by the passage of the fluidized flow, or (c) the magnitude of the hydraulic elevation was lessened by some permanent ductile straining of the overburden. Based on the easily compactable clay-rich nature of the host sediments, we prefer the latter explanation, and note that Shoulders et al. (2007) describe considerable localised deformation of the crestal regions of some forced folds (cf. Frey Martinez et al., 2007).

Much further work is required on this topic, but the limited results presented here illustrate the potential for estimating the intrusive volume directly from the deformation of the 'overburden,' and this is potentially of considerable value in the analysis of petroleum traps whose reservoirs are developed entirely as intruded sandstones (e.g. Volund Field; de Boer et al., 2007).

6.4. Implications for basin hydrodynamics

The widespread development of conical sandstone intrusions in the North Sea and Faeroe–Shetland Basins has profound implications for the hydrodynamic evolution of these post-rift basins. In the previous discussion, we have followed previous studies in assuming that sandstone dykes and sills are filled mode I fractures (Fyfe et al., 1978; Gretener, 1980; Lorenz et al., 1991; Cosgrove, 2001; Jolly and Lonergan, 2002). Once the fracture has formed, the fracture walls must be held open by the fluid pressure of the fluidized sand (P_f). From this, we can simply write that $P_f > \sigma_{min}$, where σ_{min} is the minimum confining stress acting on the fracture wall. Note that this expression simply eliminates any strength (Jolly and Lonergan, 2002) or stress intensity (Engelder and Lacazette, 1990) factors because it is an expression for a dynamic equilibrium of the pressurised crack. This means that for flat-based sandstone intrusions with concordant bases intruded along shallow-dipping bedding surfaces for example, P_f must have been greater than the vertical stress (σ_v) during the inflation phase of aperture widening. For conical intrusions, the opening direction is likely to be vertical because of the close relationship between the shapes of the forced domal folds and the aperture variation in the intrusions, and this too, argues that P_f must have been greater than the vertical stress (σ_v).

The implications of the intruding fluidized sand having a greater than lithostatic pressure are shown using a schematic pressure-depth plot based on the intrusion complex in the Faeroe–Shetland Basin (Fig. 14). This shows that the parent units from which the deepest conical intrusions were derived must have had a fluid pressure above the local lithostatic value during the main intrusion phase, because almost flat lying sills are observed to emanate directly from the parent body (Shoulders and Cartwright, 2004). The deeper level conical intrusions are mapped as feeding successively shallower level cones over a vertical distance of 700 m, and at each cone the same condition of $P_f > \sigma_{min}$ must apply. The fluid pressure profile through the nested cone / wing / dyke complexes must therefore satisfy two conditions; to keep the system open it must (1) lie above the relevant fracture closure stress at all levels, and (2) must also maintain a continuous path of decreasing fluid potential to allow upwards flow. Since we argue that conical intrusions must lift the overburden during their intrusion, P_f must have been greater than the vertical stress (σ_v). It is evident, therefore, that the fluid pressure of the interconnected intrusion network during the intrusion event must follow an upward trajectory on the pressure–depth plot that lies either on (an extreme minimum case), or somewhere above (a more likely case) the lithostatic gradient. Given this lithostatic fluid pressure condition, this might explain the lack of any preferred intrusion along polygonal faults in the host

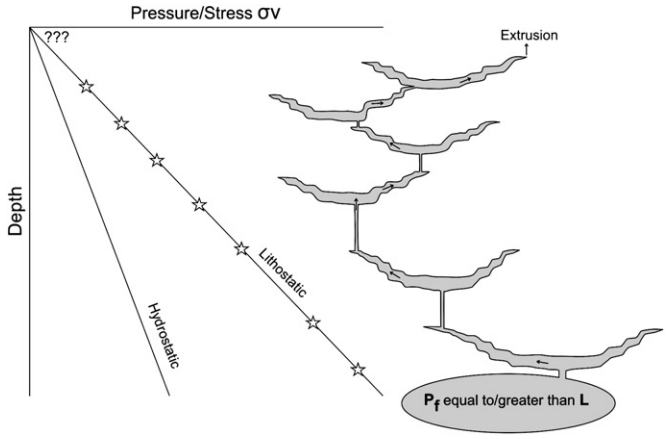

Fig. 14. Schematic pressure-depth plot for the intrusion complex in the Faeroe–Shetland Basin, during peak conditions of flow once the fracture network had formed. The pore fluid pressure in the parent body is inferred to have been equal to or greater than lithostatic because sills are observed to emanate from the top of this unit (Shoulders et al., 2007). The star symbols represent the minimum fluid pressures required in the overlying interconnected conical intrusions to keep open a continuous conduit and to permit flow from the parent body to the top of the intrusion complex.

units, because the greater the fluid pressure, the less the dependence on any in situ mechanical anisotropy (Delaney et al., 1986). By analogy, similar conditions could have applied in the intrusive complexes of the North Sea Basin. This places very specific constraints on the pre-conditioning and triggering mechanisms leading to such large scale sandstone intrusion in both basins.

The recognition that the driving condition for conical intrusions in these basins involved the build-up of pore fluid pressure to values above lithostatic raises a number of fundamental questions for future research in this field. First, what mechanisms can lead to such an extreme overpressuring for parent sand bodies of such large lateral extent (>1000s km^2)? Second, was the extreme overpressuring itself a factor in the development of the dominant conical geometry of the intrusions? Could, for example, pressure gradients between parent body and the surface have been so large as to result in such an energetic propagation that a conical geometry is developed through percussive fracturing modes? Finally, are these conditions so specific, that conical intrusions will only be expected to form in a small number of basins, or could they be far more widespread than our current data limits us to document?

7. Conclusions

1. Two geometrical end members for large conical sandstone intrusions are recognised in the North Sea and Faeroe–Shetland Basins: ‘apical cones’ and ‘flat-based bowls.’
2. These exhibit strong similarity with bowl-shaped igneous sills.
3. Both end members are associated with forced domal folds that result from hydraulic elevation of the overburden.
4. Aperture of the conical sandstone intrusions is measured for the first time on seismic data using reflections from the upper and lower boundaries of the intruded bodies, and is seen to taper away to the tips of the inverted cones.
5. Measurements of structural relief accord well with the measurements of sandstone intrusion aperture implying a direct relationship between the two parameters and strongly supporting the interpretation of sill-like emplacement. This method has predictive potential in petroleum exploration.
6. Apical cones are suggested to form by a process analogous to the formation of cone sheets.
7. Flat-based bowls are suggested to result from interactions of a laterally propagating concordant sheet with the free surface, in direct analogy with the model for equivalent igneous intrusions proposed by Pollard and Holzhausen (1979).
8. Two end-member models are presented for aperture growth during propagation but these require further testing with additional data.

Acknowledgements

R. Weinberg and S. Paterson are thanked for thoughtful and constructive reviews. Exxon-Mobil and Tranche 6 partners are thanked for permission to publish seismic data from the Faeroe–Shetland Basin. David Pollard, Jon Olsen, Martin Jackson, Wytze de Boer and Frank Peel are thanked for valuable discussions. Tom Praeger and Kuncho Kurtev are thanked for help with the figures. The paper was largely written whilst one of us (J.A.C.) was a Jackson Distinguished Visiting Fellow at the Bureau of Economic Geology, University of Texas, Austin, and its Director, Scott Tinker, and staff are acknowledged for their hospitality and support.

References

Anderson, E.M., 1936. The dynamics of the formation of cone-sheets, ring-dykes and cauldron-subsidences. Proceedings of the Royal Society of Edinburgh 56, 128–157.
Bailey, E.B., Clough, C.T., Wright, W.B., Ritchie, J.E., Wilson, G.V., 1924. The tertiary and post-tertiary geology of Mull. Geological Survey of Scotland. Memoir, 445.
Boehm, A., Moore, J.C., 2002. Fluidised sandstone intrusions as an indicator of Paleostress orientation, Santa Cruz, California. Geofluids 2, 147–161.
Branney, M.J., 1995. Downsag and extension at calderas. Bulletin of Volcanology 57, 303–318.
Brown, A.R., 2003. Interpretation of three dimensional seismic data. AAPG Memoir 42.
Cartwright, J.A., 1994. Episodic basin-wide hydrofracturing of overpressured Early Cenozoic mudrock sequences in the North Sea Basin. Marine and Petroleum Geology 11, 587–607.
Cartwright, J.A., Dewhurst, D., 1998. Layer-bound compaction faults in fine-grained sediments. Bulletin of the Geological Society of America 110, 1242–1257.
Cartwright, J.A., Hansen, D.M., 2006. Magma transport through the crust via interconnected sill complexes. Geology 34, 929–932.
Chang, 2004. Experimental hydraulic fracture. PhD thesis, Georgia Technical University, Atlanta, GA.
Cosgrove, J., 2001. Hydraulic fracturing during the formation and deformation of a basin: a factor in the dewatering of low-permeability sediments. AAPG Bulletin 85, 737–748.
Cosgrove, J., Hillier, R.D., 2000. Forced fold development within Tertiary sediments of the Alba Field, UKCS: evidence of differential compaction and post-depositional sandstone remobilization. In: Cosgrove, J., Ameen, M.S. (Eds.), Forced Folds and Fractures. Special Publication, vol. 169. Geological Society, London, pp. 61–71.
Dake, L.P., 2001. The Practice of Reservoir Engineering. Developments in Petroleum Science. Elsevier, Amsterdam.
De Boer, W., Rawlinson, P.B., Hurst, A., 2007. Successful exploration of a sand injectite complex: Hamsun prospect, Norway block 24/9. In: Hurst, A., Cartwright, J.A. (Eds.), Sand Injectites: Implications for Hydrocarbon Exploration and Production, AAPG, Memoir 87, pp. 65–68.
Delaney, P.T., Pollard, D.D., Ziony, J.I., McKee, E.H., 1986. Field relations between dykes and joints: emplacement processes and paleostress analysis. Journal of Geophysical Research 91, 4920–4938.
Dixon, R.J., Schofield, K., Anderton, R., Reynolds, A.D., Alexander, R.W.S., Williams, M.C., Davies, K.G., 1995. Sandstone diapirism and clastic intrusion in the Tertiary submarine fans of the Bruce-Beryl Embayment, Quadrant 9, UKCS. In: Hartley, A.J., Prosser, D.J. (Eds.), Characterisation of Deep-marine Clastic Systems. Special Publication, vol. 94. Geological Society, London, pp. 77–94.
Duranti, D., Hurst, A., 2004. Fluidisation and injection in the deep-water sandstones of the Eocene Alba Formation (UK North Sea). Sedimentology 51, 503–529.
Duranti, D., Hurst, A., Bell, C., Groves, S., 2002. Injected and remobilised sands of the Alba Field (UKCS): sedimentary facies characteristics and wireline log responses. Petroleum Geoscience 8, 99–107.
Engelder, T., Lacazette, A., 1990. Natural hydraulic fracturing. In: Barton, N., Stephansson, O. (Eds.), Rock Joints: Proceedings of the International Symposium on Rock Joints. A.A. Balkema, Brookfield, VT, pp. 35–43.
Fialko, Y., Kazan, Y., Simons, M., 2001. Deformation due to a pressurized horizontal circular crack in an elastic half-space, with applications to volcano geodesy. Geophysical Journal International 146, 181–190.
Frey-Martinez, J.M., Cartwright, J.A., Hall, B., Huuse, M., 2007. Clastic intrusion at the base of deepwater sands: a trap forming mechanism in the Eastern Mediterranean. In: Hurst, A., Cartwright, J.A. (Eds.), Sand Injectites: Implications for Hydrocarbon Exploration and Production. AAPG Memoir, 87, pp. 49–64.
Fyfe, W.S., Price, N.J., Thomson, A.B., 1978. Fluids in the Earth’s Crust. Elsevier, New York, 383 pp.

Galland, O., d'Ars, J., Cobbold, P.R., Hallot, E., 2003. Physical models of magma intrusion during thrusting. Terra Nova 15, 405–409.
Gallo, F., Woods, A.W., 2004. On steady homogeneous sand-water flows in a vertical conduit. Sedimentology 51, 195–210.
Gras, R., Cartwright, J.A., 2002. 3D seismic analysis of sandstone intrusions. European Association of Petroleum Geologists Annual Meeting, Florence. Extended Abstracts, H020.
Gretener, P.E., 1980. Pore pressure: fundamentals, general ramifications, and implications for structural geology (revised). AAPG Education Course Notes Series 4, 131.
Gudmundsson, A., 2002. Emplacement and arrest of sheets and dykes in central volcanoes. Journal of Volcanological and Geothermal Research, 279–298.
Hansen, D.M., 2004. 3D seismic characterisation of igneous sill complexes in sedimentary basins. PhD thesis, Cardiff University, Cardiff, UK, 312 pp.
Hansen, D.M., Cartwright, J.A., Thomas, D., 2004. 3D seismic analysis of the geometry of igneous sills and sill intersecting relationships. In: Davies, R.J., Cartwright, J., Stewart, S.A., Underhill, J.R., Lappin, M. (Eds.), 3D Seismic Technology: Application to the Exploration of Sedimentary Basins. Memoir, vol. 29. Geological Society, London, pp. 199–208.
Hansen, D., Cartwright, J.A., 2006a. Saucer-shaped sill with lobate morphology revealed by 3D seismic data: implications for resolving a shallow-level sill emplacement mechanism. Journal of the Geological Society, London 163. 509-523.
Hansen, D., Cartwright, J.A., 2006b. The three-dimensional geometry and growth of forced folds above saucer-shaped igneous sills. Journal of Structural Geology 28, 1520–1535.
Harker, A., 1904. The Tertiary Igneous Rocks of Skye. Geological Survey of Scotland, Memoir, 645 pp.
Hills, E.S., 1963. Elements of Structural Geology. Methuen, London, 483 pp.
Hubbert, M.K., Willis, D.G., 1957. Mechanics of hydraulic fracturing. Transactions of American Institute of Mining Engineers 210, 153–168.
Hurst, A., Cartwright, J.A., 2007. Relevance of sand injectites to hydrocarbon exploration and production. In: Hurst, A., Cartwright, J.A. (Eds.), Sand Injectites: Implications for Hydrocarbon Exploration and Production. AAPG Memoir, vol. 87, pp. 1–20.
Huuse, M., Duranti, D., Groves, S., Guargena, C., Prat, P., Holm, K., Steinsland, N., Cronin, B.T., Hurst, A., Cartwright, J.A., 2003. Sandstone intrusions: detection and significance for exploration and production. First Break 21, 33–42.
Hurst, A., Cartwright, J.A., Duranti, D., Huuse, M., Nelson, M., 2005. Sand injectites: an emerging global play in deep-water clastic environments. In: Dore, A., Vining, B. (Eds.), 6th Petroleum Geology Conference: North West Europe & Global Perspectives. Geological Society, London, pp. 133–144.
Hurst, A., Cartwright, J.A., Huuse, M., Duranti, D., 2006. Extrusive Sandstones (Extrudites): a New Class of Stratigraphic Trap. In: Special Publication, vol. 254. Geological Society of London. 289–300.
Huuse, M., Mickelson, M., 2004. Eocene sandstone intrusions in the Tampen Spur area (Norwegian North Sea Quad 34) imaged by 3D seismic data. Marine and Petroleum Geology 21, 141–155.
Huuse, M., Duranti, D., Steinsland, N., Guargena, C., Prat, P., Holm, K., Cartwright, J.A., Hurst, A., 2004. Seismic characteristics of large-scale sandstone intrusions in the Paleogene of the South Viking Graben, UK and Norwegian North Sea. In: Davies, R.J., Cartwright, J., Stewart, S.A., Underhill, J.R., Lappin, M. (Eds.), 3D Seismic Technology: Application to the Exploration of Sedimentary Basins. Memoir, vol. 29. Geological Society, London, pp. 262–277.
Huuse, M., Cartwright, J.A., Gras, R., Hurst, A., 2005. Km-scale sandstone intrusions in the Eocene of the Outer Moray Firth (UK North Sea): migration paths, reservoirs, and potential drilling hazards. In: Doré, A.G., Vining, B. (Eds.), Petroleum Geology of NW Europe: Proceedings of the 6th Conference. Geological Society, London, pp. 1577–1594.
Huuse, M., Cartwright, J.A., Hurst, A., Steinsland, N., 2007. Seismic characterisation of large-scale sandstone intrusions. In: Hurst, A., Cartwright, J.A. (Eds.), Sand Injectites: Implications for Hydrocarbon Exploration and Production. AAPG Memoir, vol. 87, pp. 21–38.
Jackson, M.D., Pollard, D.D., 1988. The laccolith-stock controversy – new results from the southern Henry Mountains, Utah. Geological Society of America Bulletin 100, 117–139.
James, D.M.D., 2003. Discussion on mechanisms and controls on the formation of sand intrusions. Journal of the Geological Society London 160, 1–3.
Jenkins, O.P., 1930. Sandstone dikes as conduits for oil migration through shales. AAPG Bulletin 14, 411–421.
Johnson, S.C., Paterson, S.R., Tate, M.C., 1999. Structure and emplacement history of the Zarza intrusive complex. Geological Society of America Bulletin 111, 607–619.
Jolly, R., Lonergan, L., 2002. Mechanisms and controls on the formation of sand intrusions. Journal of the Geological Society London 159, 605–617.
Jolly, R., Sanderson, D.J., 1997. A Mohr-circle construction for the opening of a pre-existing fracture. Journal of Structural Geology 19, 887–892.
Jonk, R., Mazzini, A., Duranti, D., Parnell, J., Cronin, B., Hurst, A., 2003. Fluid escape from reservoirs: implications from cold seeps, fractures and injected sands Part II. The fluids involved. Journal of Geochemical Exploration 78-79, 297–300.
Kavanagh, J., Menand, T., Sparks, R., 2006. An experimental investigation of sill formation and propagation in layered clastic media. Earth and Planetary Science Letters 245, 799–813.
LeBas, M., 1971. Cone-sheets as a mechanism of uplift. Geological Magazine 108, 373–376.
Lister, J., Kerr, A.C., 1992. Fluid-mechanical models of crack propagation and their application to magma transport in dykes. Journal of Geophysical Research 96, 10049–10077.
Lonergan, L., Cartwright, J.A., 1999. The role of polygonal fault systems in the reservoir geology of the Alba Field, North Sea. AAPG Bulletin 83, 410–432.
Lonergan, L., Lee, N., Johnson, H.D., Cartwright, J.A., Jolly, R.J.H., 2000. Remobilization and injection in deepwater depositional systems: implications for reservoir architecture and prediction. In: Weimer, P., Slatt, R.M., Coleman, J., Rosen, N.C., Nelson, H., Bouma, A.H., Styzen, M.J., Lawrence, D.T. (Eds.), Deep-water Reservoirs of the World. GCSSEPM Foundation, Houston, TX, pp. 515–532. 20th Annual Conference.
Lonergan, L., Borlandelli, C., Taylor, A., Quine, M., Flanagan, K.P., 2007. the three-dimensional geometry of sandstone injection complexes in the Gryphon Field, UK North Sea. In: Hurst, A., Cartwright, J.A. (Eds.), Sand Injectites: Implications for Hydrocarbon Exploration and Production, pp. 103–112. AAPG Memoir 87.
Lorenz, J.C., Teufel, L.W., Warpinski, N.R., 1991. Regional fractures I: a mechanism for the formation of regional fractures at depth in flat-lying reservoirs. AAPG Bulletin 75, 1714–1737.
Løseth, H., Wensaas, L., Arntsen, B., Hovland, M., 2003. Gas and fluid injection triggering shallow mud remobilisation in the Hordaland Group, North Sea. In: Van Rensburgen, P., Hillis, R.R., Maltman, A.J., Morley, C.K. (Eds.), Subsurface Sediment Mobilization. Special Publications, vol. 216. Geological Society, London, pp. 139–158.
MacLeod, M.K., Hanson, R.A., Bell, C.R., McHugo, S., 1999. The Alba Field ocean bottom cable seismic survey: impact on development. The Leading Edge 18, 1306–1312.
Malthe-Sørensen, A., Planke, S., Svensen, H., Jamtveit, B., 2004. Formation of Saucer-Shaped Sills. In: Special Publication, vol. 234. Geological Society, London. 215-227.
Mandl, G., 2000. Faulting in Brittle Rocks. Springer, Berlin.
Molyneux, S.J., 2001. Sandstone remobilisation in the Eocene to Miocene of the central and northern North Sea. PhD thesis, University of London.
Molyneux, S.J., Cartwright, J.A., Lonergan, L., 2002. Conical amplitude anomalies as evidence for large scale sediment intrusions. First Break 20, 123–129.
Murdoch, L.C., 2002. Mechanical analysis of idealized shallow hydraulic fracture. Journal of Geotechnical and Geoenvironmental Engineering 128, 488–495.
Newsom, J.F., 1903. Clastic dykes. Geological Society of America Bulletin 14, 227–268.
Newton, S.K., Flanagan, K.P., 1993. The Alba Field: evolution of the depositional model. In: Parker, J.R. (Ed.), Petroleum Geology of NW Europe, Proceedings of the 4th Conference. Geological Society, London, pp. 161–171.
O'Rourke, T.D., Turner, S.M., 1981. Empirical methods for estimating subsidence in US coalfields. Proceedings of the 22nd US Symposium on Rock Mechanics, 322–327. MIT.
Pollard, D.D., 1973. Derivation and evaluation of a mechanical model for sheet intrusions. Tectonophysics 19, 233–269.
Pollard, D.D., Holzhausen, G., 1979. On the mechanical interaction between a fluid-filled fracture and the earth's surface. Tectonophysics 53, 27–57.
Pollard, D.D., Johnson, A.M., 1973. Mechanics of growth of some laccolithic intrusions in the Henry Mountains, Utah, II: bending and failure of overburden layers and sill formation. Tectonophysics 18, 311–354.
Pollard, D.D., Muller, O.H., Dockstader, D.R., 1975. The form and growth of fingered sheet intrusions. Bulletin of the Geological Society of America 86, 351–363.
Polteau, S., Mazzini, A., Galland, O., Planke, S., Malthe-Sorenssen, A., 2008. Saucer-shaped intrusions: occurrences, emplacement and implications. Earth and Planetary Science Letters 266, 195–204.
Rubin, A.M., 1995. Propagation of magma filled cracks. Annual Reviews of Earth and Planetary Sciences 23, 287–336.
Shoulders, S., 2005, Mechanics of Sandstone Intrusions. PhD thesis, Cardiff University, Cardiff, UK, 287 pp.
Shoulders, S., Cartwright, J.A., 2004. Constraining the depth and timing of large-scale conical sandstone intrusions. Geology 32, 661–665.
Shoulders, S., Cartwright, J.A., Huuse, M., 2007. Sandstone intrusions and polygonal faults in the Faeroe-Shetland Basin. Marine and Petroleum Geology 24, 173–188.
Smallwood, J., Maresh, J., 2002. The properties, morphology and distribution of igneous sills: modelling, borehole data and 3D seismic from the Faroe–Shetland area. In: Jolley, D.W., Bell, B.R. (Eds.), The North Atlantic Igneous Province: Stratigraphy, Tectonic, Volcanic and Magmatic Processes. Special Publication, vol. 197. Geological Society, London, pp. 271–306.
Stuevold, L., Faerseth, R., Arnsen, L., Cartwright, J.A., Moller, N., 2003. Polygonal faults in the Ormen Lange Field, offshore Norway. In: van Rensbergen, R., Hillis, A., Maltman, A., Morley, C. (Eds.), Subsurface Sediment Mobilisation. Special Publication, vol. 216. Geological Society, London, pp. 263–282.
Taylor, B.J., 1982. Sedimentary dykes, pipes and related structures in the Mesozoic sediments of Alexander Island. British Antarctic Survey Bulletin 51, 1–42.
Teige, G.M., Hermanrud, C., Wensaas, L., Bolas, H.M., 1999. The lack of relationship between overpressure and porosity in North Sea and Haltenbanken shales. Marine and Petroleum Geology 16, 321–335.
Thomson, K., Hutton, D., 2004. Geometry and growth of sill complexes: insights using 3D seismic from the North Rockall Trough. Bulletin of Volcanology 66, 364–375.
Trude, J., 2004. The mechanics of igneous sill emplacement from three-dimensional seismic data. PhD thesis, Cardiff University, p. 287.
Wilson, K.C., Addie, G.R., Sellgren, A., Clift, R., 2006. Slurry Transport Using Centrifugal Pumps. Springer, Berlin.
Witherspoon, P.A., Neuman, S.P., 1972. Hydrodynamics of fluid injection. AAPG Memoir 18, 258–272.
Yang, Y., Aplin, A.C., Larter, S.C., 2004. Quantitative assessment of mudstone lithology using geophysical wireline logs and artificial neural networks. Petroleum Geoscience 10, 141–152.